Aerosol Science and Technology
Publication details, including instructions for authors and subscription information:
http://www.tandfonline.com/loi/uast20

Modeling Multicomponent Aerosol Particle Growth By Vapor Condensation

Fred Gelbard [a]

[a] Sandia National Laboratories , Containment Modeling Division , 6429, P.O. Box 5800, Albuquerque, NM, 87185

Published online: 07 Jun 2007.

To cite this article: Fred Gelbard (1990) Modeling Multicomponent Aerosol Particle Growth By Vapor Condensation, Aerosol Science and Technology, 12:2, 399-412, DOI: 10.1080/02786829008959355

To link to this article: http://dx.doi.org/10.1080/02786829008959355

Modeling Multicomponent Aerosol Particle Growth By Vapor Condensation

Fred Gelbard
Sandia National Laboratories, Containment Modeling Division, 6429, P.O. Box 5800, Albuquerque, NM 87185

A new "moving-sectional" method is presented to solve the dynamics of multicomponent aerosol particle growth by vapor condensation in a closed system. The method controls numerical diffusion and stiffness by adapting the method of characteristics to a sectional representation of the aerosol. An exact solution for a closed system is presented, and the "moving-sectional" method gives excellent agreement when tested against this solution. Four cases are presented to demonstrate the importance of the solute, Kelvin, and latent heat effects.

INTRODUCTION

Modeling the dynamics in a nuclear reactor containment under accident conditions has posed many modeling and computational problems. Current codes, such as the CONTAIN code by Bergeron et al. (1985), are an assemblage of complex models that can simulate a wide variety of accident conditions to determine the temperature and pressure in containment. An important part of the code is the model for aerosol behavior.

The aerosol is likely to be a complex mixture of soluble and insoluble material in the possible presence of steam. Some of the aerosol material may be highly radioactive and thus of concern for its possible health consequences. Since particle size and composition are important variables for determining the respirability and health effects of an aerosol, a sectional model was developed by Gelbard and Seinfeld (1980) to track chemical species as a function of particle size and time. This sectional model is the basis for the CONTAIN aerosol module.

The sectional model was found to be robust for aerosol sources, and particle coagulation and deposition processes. The original sectional model, however, was not robust at high condensation or evaporation rates. Improvements were later made in CONTAIN 1.1 by Murata et al. (1988) to resolve this problem. In particular, the calculation of rapid aerosol evaporation was modified to utilize the method of characteristics, similar to the approach developed for this work. However, CONTAIN did not use that method for modeling condensation, and did not include the solute or Kelvin effects.

The present paper describes a method of characteristics for the general problem of a closed system of aerosol and condensable vapor including the solute and Kelvin effects. The method is called the "moving-sectional" technique and is applied to problems without particle coagulation, deposition, and sources. The method is similar to the standard sectional approach in that the particle size domain is divided into m size classes called sections. Within each section the aerosol particles are approximated as having the same chemical composition. However, as the name of the method implies, the sections are no longer fixed in time, but will move. This extra degree of freedom was shown by Gelbard (1987) to greatly improve the accuracy of the calculation. With a moving-sectional algorithm, the CONTAIN code

Aerosol Science and Technology 12:399–412 (1990)
Published by Elsevier Science Publishing Co., Inc.

0278-6826/90/$0.00

readily modeled the dramatic effects of a hydrogen burn on a wet soluble aerosol in containment.

Because of the complexity of containment modeling, basic aerosol processes could not be easily isolated to determine their influence on the aerosol. Therefore, this work presents the theoretical basis for the moving-sectional method, independent of the other models associated with containment modeling, and independence of aerosol particle coagulation, deposition, and sources. To test the method, a new exact solution for simplified particle growth rates is developed and compared to the moving-sectional solution. Finally, four applications of the method are presented to assess the importance of the solute effect, the Kelvin effect, and the effect of heat released by vapor condensation.

BACKGROUND

The governing mass and energy balances for a closed system of aerosol and condensable vapor are

$$\frac{\partial n(v,t)}{\partial t} + \frac{\partial [I(v,t)n(v,t)]}{\partial v} = 0 \qquad (1)$$

$$C = Q_s(t) + \int_0^\infty v n(v,t)\,dv \qquad (2)$$

$$MC_v(T - T_0) = \Delta H[Q_s(0) - Q_s(t)], \qquad (3)$$

where $n(v,t)$ is the number density function of particles of mass v at time t, $I(v,t)$ is the particle growth rate of a particle of mass v, Q_s is the condensable vapor mass concentration, C is a constant equal to the total mass concentration of aerosol particles and condensable vapor, M is the suspending gas mass concentration, C_v is the suspending gas specific constant volume heat capacity, T is the temperature, and ΔH is the specific energy released by condensation. In the energy balance given by Eq. (3), the thermal capacity of the aerosol particles is neglected since it is much less than that for the suspending gas.

In previous analytical work by Brock (1971, 1983), Gelbard and Seinfeld (1979), and Williams (1983), Eqs. (2) and (3) were neglected and isothermal conditions were assumed. The condensable vapor concentration was assumed to be either constant or prescribed independently. However, for a closed system, $I(v,t)$ is temperature dependent and intimately coupled to Q_s. Thus $n(v,t)$, Q_s, and T should be determined simultaneously.

For practical applications, Eqs. (1), (2), and (3) are solved numerically. As discussed by Dunbar (1985), previous numerical solutions discretized the particle size domain into a fixed computational grid. That approach has encountered several computational difficulties.

Equation (1) is hyperbolic, and for such equations it is well known that fixed-grid solutions may lead to numerical diffusion that trends to smear sharp changes in the particle mass density function. Thus spurious particles may remain in the smallest particle size range, that have actually been swept of aerosol by condensational growth. Similarly, spurious particles may remain in the largest particle size ranges that have been swept of aerosol by evaporation. This error can be reduced by drastically refining the discretization. However, Warren and Seinfeld (1985) have shown that the computational effort for such an approach may be prohibitive.

Another problem is associated with the wide range of time scales for aerosol processes. Since the particle size domain may extend over several orders of magnitude in particle diameter, the characteristic time scales for particle growth may also have a large variation. This results in a stiff system of differential equations. Such systems require complicated solution techniques to take time steps much larger than the shortest physical time scale of the problem. These complicated solution techniques are not robust and are computationally expensive.

Furthermore, particles of the same size but of different chemical compositions are not represented with the fixed-grid sectional model. Due to the solute effect, particle

growth by vapor condensation may be highly dependent on the particle's chemical composition. Thus the variation of chemical composition for particles of the same size may be important and should be modeled.

All three of these problems of 1) numerical diffusion, 2) stiffness, and 3) chemical composition effects, are addressed in this work. Previous approaches are reviewed, and it is shown that a fixed-grid approach may never completely resolve the problems of numerical diffusion and stiffness.

PREVIOUS FIXED GRID NUMERICAL SOLUTION APPROACHES

For modeling condensational growth of an aerosol, a fixed-grid upwind differencing scheme was first reported for a multicomponent aerosol by Gelbard and Seinfeld (1980). Later, a fixed-grid central differencing and a much improved fixed-grid upwind differencing schemes were reported by Bassett et al. (1981) and, Warren and Seinfeld (1985), respectively. These schemes are more accurate than the original formulation, but are still subject to numerical diffusion and stiffness problems. A rigorous analysis of why these fixed-grid approaches could not overcome stiffness and numerical diffusion problems can be developed by studying the resulting linear differential equations for a constant condensable vapor concentration.

For a fixed grid in particle size, the differential equations for the mass concentration of particles in section i, (i.e. particle size class i), for an upwind differencing scheme is given by

$$\frac{dQ_i}{dt} = G_i Q_i + c_{i-1} Q_{i-1} - c_i Q_i \qquad i \geq 1, \tag{4}$$

where $c_0 = 0$, and c_i for $i \geq 1$ is the kinetic coefficient for aerosol mass transfer between adjacent sections, and G_i is the kinetic coefficient for vapor condensing on aerosol in section i, for $i \geq 1$. Both of these coefficients are dependent on the differencing scheme. The terms on the right-hand side of Eq. (4) represent the mass concentration increase in section i by condensation on to particles in section i, the gain of aerosol mass concentration in section i by particles growing into section i from section $i-1$, and the loss of aerosol mass concentration by particles growing out of section i, respectively. For constant condensable vapor concentration, G_i and c_i are constant with time. In matrix form, Eq. (4) reduces to

$$\frac{d\bar{Q}}{dt} = \underline{A}\bar{Q}, \tag{5}$$

where A is a matrix of the form

$$\underline{A} = \begin{bmatrix} G_1 - c_1 & & & & \\ c_1 & G_2 - c_2 & & & 0 \\ & c_2 & G_3 - c_3 & & \\ & & c_3 & \ddots & \\ & 0 & & \ddots & \\ & & & \ddots & \end{bmatrix}. \tag{6}$$

Since there are only two nonzero diagonals in $\underline{A}$, the eigenvalues of the matrix can be readily expressed as

$$\lambda_i = G_i - c_i. \tag{7}$$

Since the particle sizes of interest vary by orders of magnitude, the growth coefficients, G_i and c_i, and the difference of these coefficients may also vary by orders of magnitude. This large variation in eigenvalues is why stiffness has plagued solution techniques for modeling condensation problems.

The existence of numerical diffusion can also be shown for this case of constant condensable vapor concentration. The exact solution for the initial conditions of $Q_1 = 1$ and $Q_i = 0$ for $i > 1$ can be expressed explicitly as

$$Q_i = \sum_{j=1}^{i} \alpha_j b_i^{(j)} \exp(\lambda_j t) \qquad i = 1, \ldots, m, \tag{8}$$

where

$$b_i^{(j)} = \begin{cases} 0 & i < j \\ 1 & i = j \\ \prod_{k=j}^{i-1} \frac{c_k}{\lambda_j - \lambda_{k+1}} & i > j \end{cases} \quad (9)$$

and

$$\alpha_1 = 1 \quad (10)$$

$$\alpha_i = -\sum_{j=1}^{i-1} \alpha_j b_i^{(j)} \qquad i > 1. \quad (11)$$

For these initial conditions of no aerosol present except in the first section, there should be a finite amount of time required before aerosol grows into the largest sections. However, notice from Eq. (8) that for any positive value of t, a nonzero aerosol mass concentration may be formed in all sections. Thus even in the case where the differential equations (i.e., Eq. 4) are solved exactly, numerical diffusion still corrupts the solution by smearing aerosol mass throughout the discretized domain.

These inherent limitations of a fixed-grid approach motivated the development of the moving-sectional method. Because a full description of the aerosol composition space is also not represented with this new method, the sectional approximation that all particles in a section have the same chemical composition is still retained. However, since sections may overlap the same region in particle size, the new method does provide the capability of having particles of the same size but of different chemical compositions. The ability of the moving-sectional method to represent such an aerosol is based on a principle described below.

PARTICLE ORDERING PRINCIPLE

To represent particles of the same size but of different chemical compositions, and to reduce the number of characteristic curves needed for modeling, the moving-sectional method utilizes what will be called a "particle ordering principle." As shown in Appendix B, this principle states that when particles grow or shrink by condensation or evaporation, respectively, particles of the same initial composition will always preserve their respective ordering in total particle mass. Thus single component aerosols will always preserve particle ordering; and if the particle size domain is discretized into sections, the moving section boundaries will never cross.

However, particle ordering may not be preserved for a multicomponent aerosol. For example, in a condensing environment, small hygroscopic particles may surpass in size initially larger but insoluble particles. The sectional approximation, that all particles within a section have the same composition, imposes particle ordering only within a section. Thus as section boundaries move, particles initially within a section will remain there since they cannot grow larger or smaller than the largest or smallest particle in the section, respectively. Thus, the total number concentration of particles between section boundaries must be constant as the section boundaries move in time, regardless of the chemical composition of the aerosol.

Furthermore, by allowing the section boundaries to move, the initially smaller hygroscopic particles may overlap in size the initially larger but insoluble particles. Thus, particles of the same size but of different chemical compositions may be obtained with a moving-sectional model. The method for computing the trajectory of the section boundaries is derived below.

DERIVATION

Using the particle ordering principle, the moving-sectional technique is derived by dividing the particle size domain into a set of m size classes called sections. Within a section, the number density function is given as a function of particle mass and a single parameter that is unique to that section but may vary in time. In this work, the sectional

approximations are chosen such that

$$Q_i = \frac{N_i \ln(v_{i,u}/v_{i,l})}{(1/v_{i,l} - 1/v_{i,u})} \qquad i = 1, \ldots, m, \tag{12}$$

where Q_i and N_i are the mass and number concentrations of aerosol in section i, respectively, and $v_{i,l}$ and $v_{i,u}$ are the lower and upper particle masses of section i, respectively. As opposed to the standard sectional technique, the moving-sectional technique does not require that $v_{i,u}$ be equal to $v_{i+1,l}$. This degree of freedom is included such that particles of the same size may be composed of different chemical compositions by having sections overlap the same region in particle size. For condensation and evaporation processes only, the number concentration in a section is constant. Thus differentiating Eq. (12) with respect to time we have

$$\frac{dQ_i}{dt} = N_i F_i \qquad i = 1, \ldots, m, \tag{13}$$

where F_i is a function only of the section boundaries and their derivatives in time. The water mass balance is given by

$$C = Q_s + \sum_{i=1}^{m} Q_{i,w}, \tag{14}$$

where $Q_{i,w}$ is the aerosol water concentration in section i. Eqs. (13) and (14) represent a system of $m + 1$ equations for the mass concentrations of aerosol water in sections 1 to m given that the section boundaries are known as a function of time. Since the model was developed for only one condensing component on a multicomponent aerosol, given the initial mass and number concentrations in a section, the mass concentrations in that section at some future time may be determined from the section boundaries and Eq. (12). Thus, only the section boundaries need to be determined as a function of time to determine the section mass concentrations.

The equations for the section boundaries are given by

$$\frac{dv_i}{dt} = r(Q_s, Q_{eq}, v_i) \qquad i = 1, \ldots, 2m, \tag{15}$$

where r is the growth rate of a single particle, and Q_{eq} is the water vapor concentration in equilibrium with a particle of size v, which is a function of temperature, particle size, and composition. At equilibrium, Q_s is equal to Q_{eq} and $dv_i/dt = 0$.

Eq. (15) specifies the problem in terms of a set of coupled differential equations. Although numerical diffusion is greatly reduced by solving these equations, the system is still stiff because the time scales for particle growth may vary over many orders of magnitude. To uncouple the equations, and hence remove the stiffness problem, the following numerical method of solution was adopted.

The steam concentration, which depends on the mass of water in the aerosol, couples the set of equations given by Eq. (15). However, using a first-order implicit approach, the steam concentration may be approximated as constant over the time step, equal to its value at the end of the time step. Then Eq. (15) becomes an uncoupled set of differential equations for the section boundaries, and numerical stiffness is no longer a problem. Furthermore, with a constant value for Q_s over the time step, Eq. (15) is separable. This reduces the task of solving for $v_i(t + dt)$ to iterating on the evaluation of a single integral:

$$\Delta t = \int_{v_i(t)}^{v_i(t+dt)} \frac{dv}{r(Q_s, Q_{eq}, v)}. \tag{16}$$

Note that the integrand in Eq. (16) is singular at equilibrium. Therefore, before iterating on Eq. (16) to determine $v_i(t + dt)$, an equilibrium calculation is performed to locate the singularity, if it exists. Then all iterations on $v_i(t + dt)$ are kept to one side of the singularity.

In this work the integral given in Eq. (16) was evaluated using a Gauss-Legendre quadrature technique. The number of iterations required to evaluate the integral generally increased the closer $v_i(t + dt)$ was to its equilibrium value.

COMPARISON WITH EXACT SOLUTION

Comparison with an exact solution for a specialized form of the particle growth rate $I(v, t)$ was sought to assess the accuracy of the moving-sectional method. A general exact solution has been reported by Brock (1983) and Williams (1983) for the case in which the condensable vapor concentrations is either constant or prescribed independently. For closed systems, such as nuclear reactor containments, the vapor concentration is coupled to the aerosol dynamics and may not be specified independently. Therefore, a new exact solution was developed to simultaneously solve Eqs. (1), (2), and (3). The derivation of the exact solution is given in Appendix A.

Figures 1 and 2 show the numerical solution computed with the moving-sectional method, and the exact solution given in Ap-

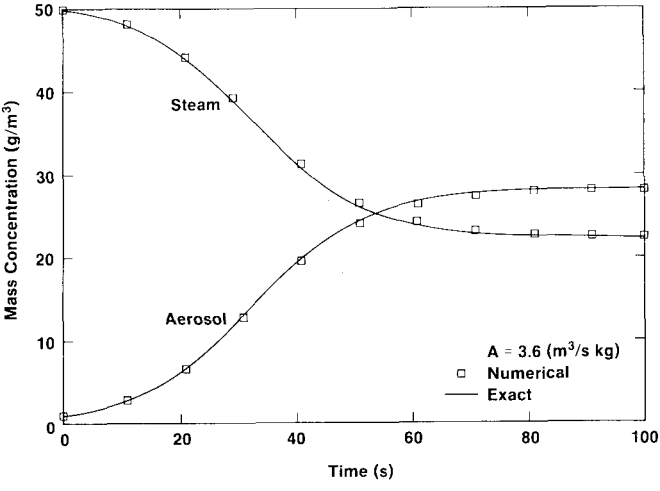

FIGURE 1. Comparison of exact and moving-sectional solutions of the steam and total aerosol mass concentrations.

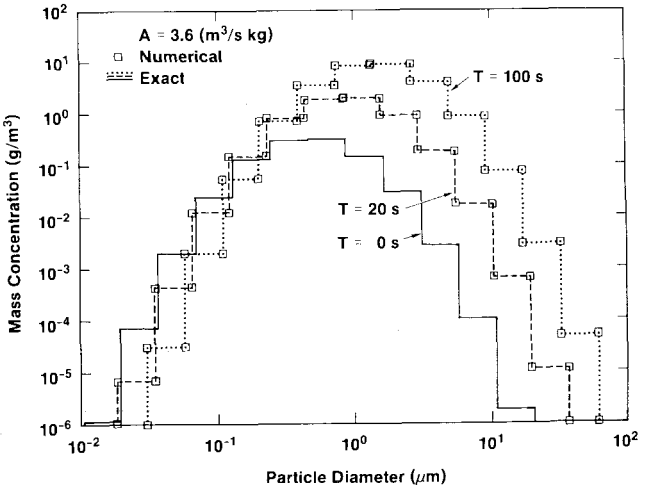

FIGURE 2. Comparison of exact and moving-sectional solutions of the aerosol mass concentrations as a function of time and particle size.

pendix A. For this case, isothermal conditions were assumed at 298 K, and the initial aerosol mass density function was lognormal with a mass median diameter of 0.1 μm and a geometric standard deviation of 1.5. The initial steam and aerosol mass concentrations were 50 and 1 g/m^3, respectively. At this steam concentration, the system was highly supersaturated since the equilibrium steam concentration at 298 K is 22.6 g/m^3. The material density of the particles was 1000 kg/m^3. The only parameter for the exact solution was the quantity A (as defined in Appendix A), a time scale parameter which was chosen as 3.6 m^3/s per kg such that equilibrium was established in about 1 min. Twelve sections and 1-s time steps were used to compute the numerical results.

Figure 1 shows the aerosol and steam mass concentrations as a function of time. Notice that excellent agreement was obtained between the numerical and exact solutions. Since the total mass concentration of aerosol is only an integral test of the moving-sectional method, a far more stringent test is the detailed comparison of section mass concentrations shown in Figure 2. Notice that excellent agreement was also obtained for the time evolution of the section concentrations, thereby demonstrating the accuracy of the moving-sectional method.

SAMPLE CALCULATIONS

Numerical calculations are required for arbitrary particle size, temperature, and chemical composition dependent particle growth rates. To demonstrate the moving-sectional method for such cases, the same initial steam and aerosol mass distribution as shown in Figure 2 was used in four cases to simulate the solute, the Kelvin, and the latent heat effects. Table 1 summarizes the phenomena considered in the four sample calculations. Figures 3 through 10 show the section boundaries and section mass concentrations for the four cases. Figure 11 shows the mass concentrations of steam and aerosol with time for all the cases.

TABLE 1. *Cases Considered in Figures 3–11.*

Case	Mechanisms			Figures
	Solute	Heat	Kelvin	
I	Neglected	Neglected	Neglected	3, 4, 11
II	Included	Neglected	Neglected	5, 6, 11
III	Included	Included	Neglected	7, 8, 11
IV	Included	Included	Included	9, 10, 11

In all four sample calculations the time step was increased geometrically by a factor of 2.0 after each time step. Increasing the time step during the calculation made it possible to simulate large time-scale variations without requiring an excessive number of time steps. About 35 time steps were required to reach equilibrium. Convergence was checked by repeating the calculation with the time step increasing geometrically by a factor of 1.5. With this smaller geometric factor, about 60 time steps were required to simulate the same time period. In all four cases no significant differences were noted in the aerosol evolution between using a geometric factor of 2.0 or 1.5.

Throughout these calculations, Mason's equation (1971), as corrected for noncontinuum effects given by Pruppacher and Klett (1980), was used to determine the particle growth rate. Accounting for the noncontinuum effects resulted in modifications to the thermal conductivity of air and the diffusivity of water vapor. However, for cases I and II, the system was isothermal and no heat effect correction was included in Mason's equation for particle growth. Mason's equation used in this work is given by

$$\frac{dv}{dt} = \frac{2\pi D\rho_w \left\{ \frac{Q_s}{Q_{eq}} - a_w \exp\left[\frac{4\sigma M_w}{RT\rho_w D} \right] \right\}}{\frac{\rho_w}{Q_{eq} D'} + \frac{\Delta H \rho_w}{k'T} \left[\frac{\Delta H M_w}{RT} - 1 \right]} \tag{17}$$

where D is the particle diameter, a_w is the activity of water, σ is the surface tension, R is the ideal gas constant, ρ_w is the density of water, M_w is the molecular weight of water,

k' is the corrected thermal conductivity of air, and D' is the corrected diffusivity of water vapor.

Figure 3 shows the section boundaries as a function of time without the solute, the Kelvin, or the latent heat effects. Notice that the smallest submicron particles, which have the shortest (submillisecond) characteristic time scale, grew very rapidly, and depleted steam until equilibrium was established. Since the large particles had a relatively long time scale, the small particles had already reduced the steam concentration to its equilibrium value before the large particles had an opportunity to grow. Figure 4 shows that the aerosol mass distribution had rapidly compressed in about 1.5 ms, and was indistinguishable from the equilibrium distribution attained at 200 s of simulation.

From Figure 3 note that the section boundaries define the region in particle size that contain aerosol. No aerosol exists below or above the smallest or largest section boundaries, respectively. Thus Figure 4 does not display numerical diffusion of aerosol beyond these boundaries. In a fixed-grid so-

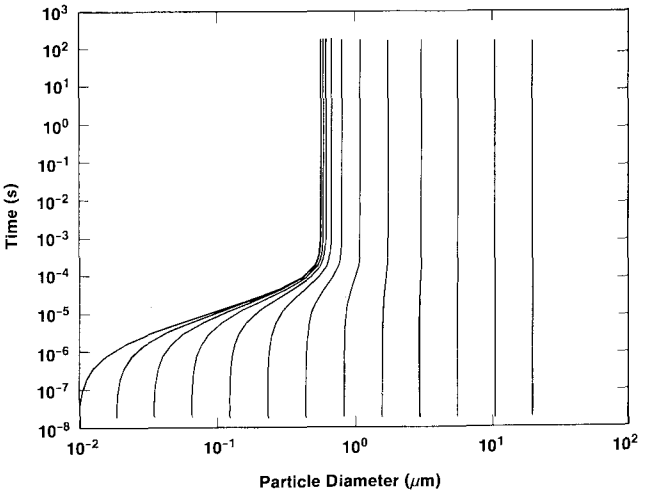

FIGURE 3. Case I: section boundaries for aerosol particle growth neglecting the solute and Kelvin effects, and the latent heat of condensation.

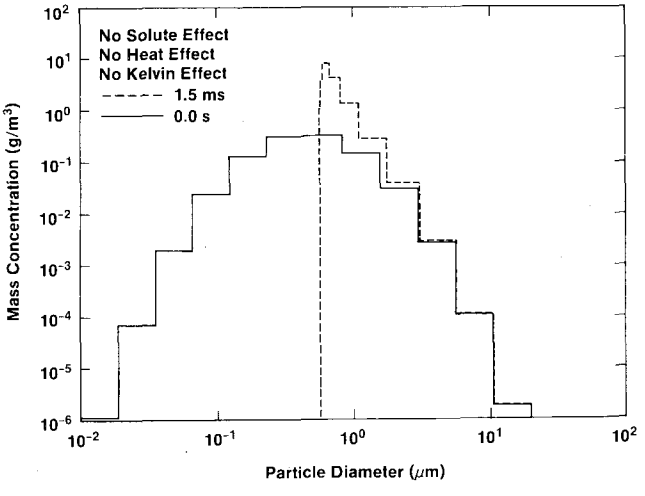

FIGURE 4. Case I: aerosol mass concentrations neglecting the solute and Kelvin effects, and the latent heat of condensation. Mass concentrations at 1.5 ms and 200 s are indistinguishable.

lution technique, however, as the aerosol evolves, spurious aerosol particles may remain in the particle size range below that given by the smallest moving-section boundary.

To model the solute effect, the initial aerosol was assumed to be composed of a soluble salt with a molecular weight of 100 g/g mol. An ideal solution of salt and water was assumed in which the water vapor pressure in solution was equal to the mole fraction of water times the vapor pressure of pure water at the same temperature. Figure 5 shows that for this ideal solution, the small aerosol particles began to grow rapidly. The smallest particles grew beyond their equilibrium size at 1 ms, because they depleted more steam than would have been available if the larger particles had the opportunity to grow. This was due to the relatively short characteristic time scales of the small particles in the aerosol. Thus in Figure 6 we see that at 1.5 ms, the aerosol mass distribution was compressed and was similar in appearance to that shown in Figure 4 without the solute effect. However with the solute effect, at about 1 ms the larger particles started their growth and depleted steam from the atmosphere. Figure 11 shows that the steam concentration at 1 ms was already reduced to its equilibrium value by the rapid growth of the small particles. Thus for the large particles to grow, water was transferred from the small particles through the atmosphere and on to the large but slower growing particles. This water transfer resulted in the small particles shrinking and the lower section boundaries reversing direction at about 1 ms as shown in Figure 5. Thus Figure 6 shows that the mass distribution first compressed and then expanded as particles approached their equilibrium size with the small particles shrinking and the large particles growing. Equilibrium was essentially achieved after about 100 s of simulation. Note from Figures 6 and 11 that although the steam and total aerosol mass concentrations may have achieved their equilibrium values within a millisecond, the aerosol still evolved and reached complete equilibrium much later, on the order of 100 s of simulation. Also note from Figure 11 that when the solute effect was included, slightly more water was condensed on the aerosol compared to case I without the solute effect.

Figures 7 and 8 show the aerosol evolution when the heat of condensation was included. As in case II without the heat effect, the aerosol mass distribution rapidly compressed and then gradually expanded. However, including the heat of condensation raised the temperature which raised the equi-

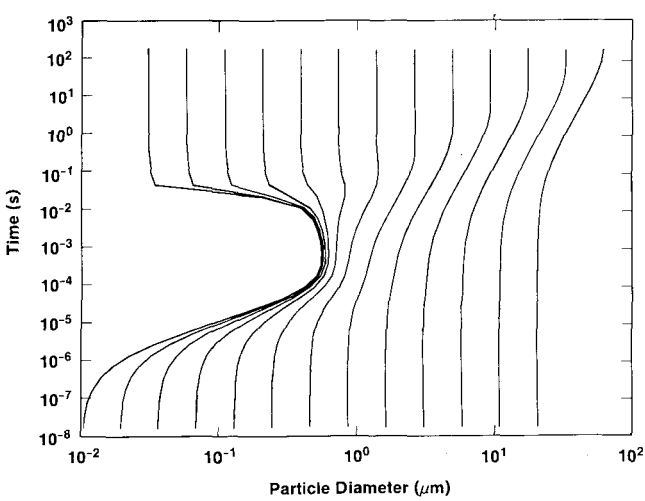

FIGURE 5. Case II: section boundaries for aerosol particle growth including the solute effect, but neglecting the Kelvin effect and the latent heat of condensation.

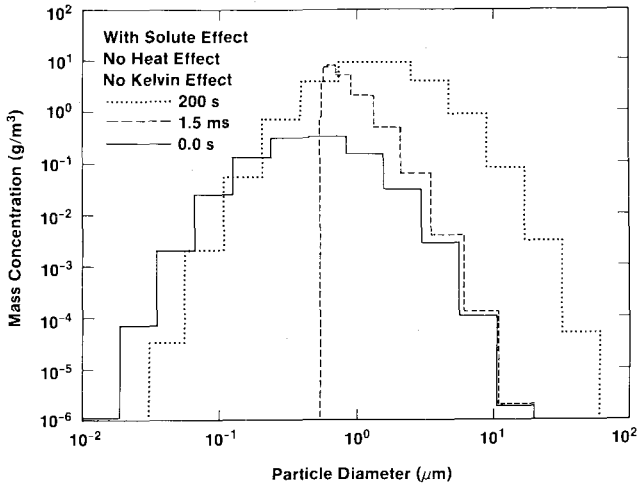

FIGURE 6. Case II: aerosol mass concentrations including the solute effect, but neglecting the Kelvin effect and the latent heat of condensation.

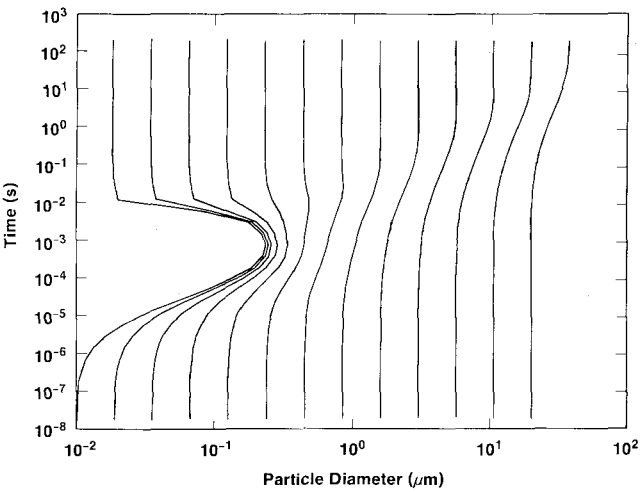

FIGURE 7. Case III: section boundaries for aerosol particle growth including the solute effect and the latent heat of condensation, but neglecting the Kelvin effect.

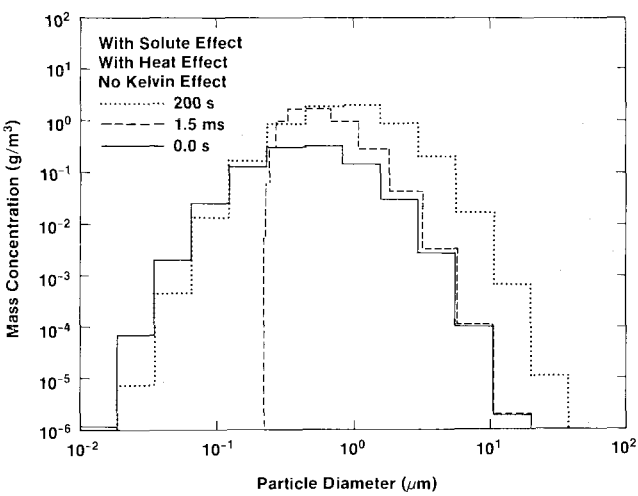

FIGURE 8. Case III: aerosol mass concentrations including the solute effect and the latent heat of condensation, but neglecting the Kelvin effect.

librium water vapor pressure above the particle, and therefore retarded particle growth. This resulted in aerosol behavior similar to that in case II without the heat of condensation effect. However, the heat effect reduced the overall aerosol growth as shown in Figure 11.

Finally, Figures 9 and 10 show the influence of the Kelvin effect. No significant differences were noted on the total condensed steam concentration with this effect. Comparing Figures 7 and 9, a slight reduction in particle size for the very smallest particle sizes can be observed with the Kelvin effect.

CONCLUSION

Several problems have been addressed by extending the fixed-grid sectional technique to allow section boundaries to move. Primarily, stiffness and numerical diffusion are no longer significant problems for modeling condensation on aerosols. By uncoupling the differential equations for the section boundaries, numerical stiffness has been resolved, and hence computational stability is greatly improved. Furthermore, with previous methods, numerical diffusion may distort the solution by leaving spurious particles in sec-

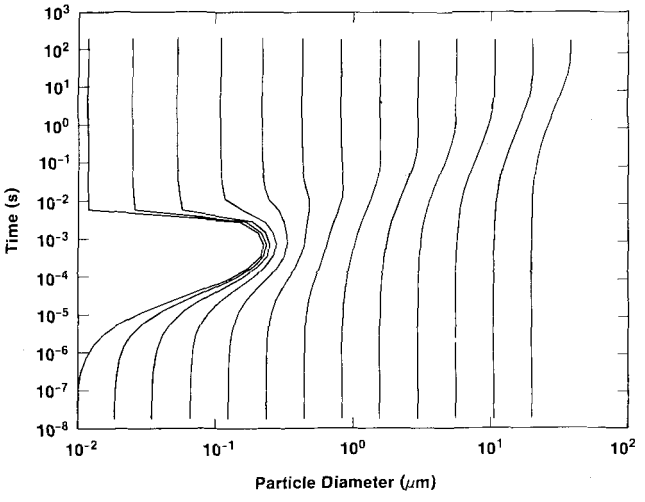

FIGURE 9. Case IV: section boundaries for aerosol particle growth including the solute and Kelvin effects, and the latent heat of condensation.

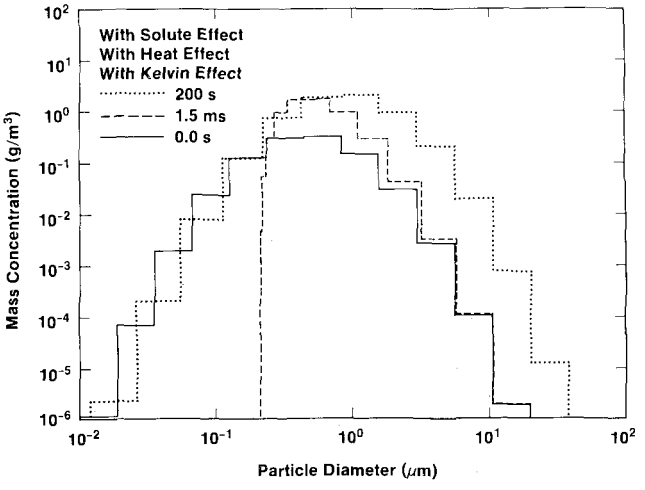

FIGURE 10. Case IV: aerosol mass concentrations including the solute, the Kelvin effect, and the latent heat of condensation.

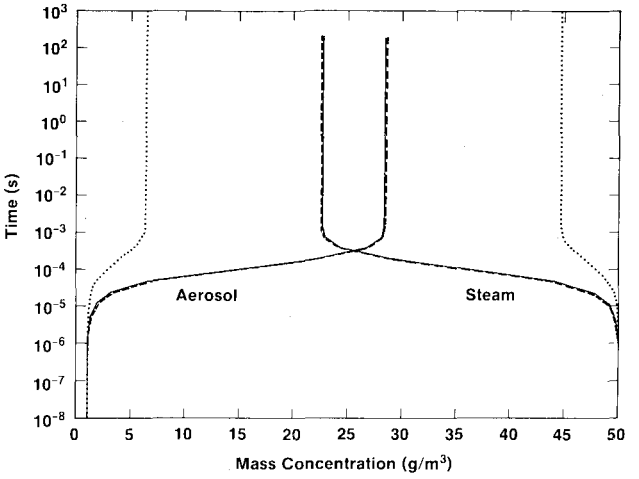

FIGURE 11. Total aerosol and steam mass concentrations for case I (*solid lines*), case II (*dashed lines*), and cases III and IV (*dotted lines*).

tions that should have been swept of aerosol by condensation/evaporation. The moving-sectional approach reduces that error to the level of discretization by adapting the method of characteristics to the problem.

An exact solution has been developed for a closed system, and the method has been successfully tested against this solution with excellent agreement. For more physically realistic particle growth rates, it was shown that the smallest particles grow rapidly. But with the solute effect included, these small particles will gradually lose their water to the slower growing larger particles. Thus the particle mass distribution may be compressed followed by a gradual expansion. With soluble aerosol particles present, the Kelvin effect did not significantly influence aerosol behavior. The heat of condensation did retard the amount of water condensed, and hence retard particle growth. However, the overall features of the mass distribution compressing and expanding were still observed with the heat and solute effects included.

APPENDIX A

Exact Solution for a Growing Aerosol in a Closed System

Williams (1983) presented a comprehensive analytical study of aerosol particle growth by vapor condensation. That work will serve as the basis for developing an exact solution for a closed system of aerosol and condensable vapor.

Using the notation given by Williams, $I(v,t)$, the particle growth rate is restricted to functional forms given by $H(t)f(v)$. In this special case, Williams found that the general solution to Eq. (1) is given by

$$f(v)n(v,t) = f\{F^{-1}[F(v)+G(0)-G(t)]\} \times n_0\{F^{-1}[F(v)+G(0)-G(t)]\}, \tag{A-1}$$

where

$$n_0(v) = n(v,0), \tag{A-2}$$

$$F(v) = \int \frac{dv}{f(v)}, \tag{A-3}$$

$$G(t) = \int H(t)\,dt, \tag{A-4}$$

and F^{-1} is the inverse function of the function F, and H is an arbitrary function of time. However, for a closed system, H may not only be a function of time, but is intimately coupled to $n(v,t)$ and T through Eqs. (2) and (3), and may not be specified arbitrarily.

To account for this coupling, the particle growth rate may be expressed as $I(v,t) =$

$A(Q_s - Q_{eq})\ f(v)$, where A is a constant. For small temperature variations, Q_{eq} may be linearly related to T, and given by $Q_{eq} = Q_{eq0} + S(T - T_0)$, where Q_{eq0} and S are constants. To obtain an exact solution, $f(v)$ will be given by v, and the Kelvin effect will be neglected. Then

$$H(t) = p + qM_1, \tag{A-5}$$

where

$$p = A\left[C - Q_{eq0} - \frac{S\Delta H}{MC_v}[Q_s(0) - C]\right], \tag{A-6}$$

$$q = -A\left[1 + \frac{S\Delta H}{MC_v}\right], \tag{A-7}$$

$$G(t) = pt + q\int M_1(t)\,dt, \tag{A-8}$$

and

$$M_1(t) = \int_0^\infty vn(v,t)\,dv. \tag{A-9}$$

Substituting Eqs. (A-8) and (A-9) into Eq. (A-1) results in

$$n(v,t) = g(t)n_0(g(t)v) \tag{A-10}$$

where

$$g(t) = \exp\left[-q\int_0^t M_1(t)\,dt - pt\right], \tag{A-11}$$

and

$$M_1(t) = M_1(0)/g(t). \tag{A-12}$$

Eqs. (A-11) and (A-12) may be combined into a single integral equation for $M_1(t)$. Differentiating that integral equation with respect to time results in

$$\frac{dM_1}{dt} = pM_1 + qM_1^2. \tag{A-13}$$

Integrating Eq. (A-13) results in

$$\frac{1}{g(t)} = \frac{M_1(t)}{M_1(0)} = \frac{pe^{pt}}{qM_1(0)\{1 - e^{pt}\} + p}. \tag{A-14}$$

The mass concentration of aerosol in section i, Q_i is given by

$$Q_i(t) = \int_{v_{i-1}}^{v_i} vn(v,t)\,dv = \int_{v_{i-1}}^{v_i} vg(t)n_0(g(t)v)\,dv. \tag{A-15}$$

This expression conveniently reduces to an expression for the mass concentration in a section which is independent of the initial mass density function within the section. Thus, the exact moving-sectional solution is

$$Q_i(t) = Q_i(0)/g(t), \tag{A-16}$$

where Eqs. (A-14) and (A-16) provide the exact solution used in Figures 1 and 2 with $S = 0$.

APPENDIX B

Proof of Particle Ordering Principle

Assume that for some $v = v^*$, v_1 approaches v_2. Then expanding $I(v,t)$ at $v = v^*$ results in

$$\frac{dv_1}{dt} = I(v^*,t) + \left.\frac{\partial I}{\partial v}\right|_{v^*}(v_1 - v^*) + \cdots \tag{B-1}$$

$$\frac{dv_2}{dt} = I(v^*,t) + \left.\frac{\partial I}{\partial v}\right|_{v^*}(v_2 - v^*) + \cdots \tag{B-2}$$

Since we are only interested in the expansion when the difference between v_1 and v_2 is small, we will retain only the first term in the expansion. Subtracting Eq. (B-1) from Eq. (B-2) and integrating results in

$$v_1 - v_2 = Z\exp(Bt), \tag{B-3}$$

where Z is a constant and B is the derivative of $I(v,t)$ with respect to v at $v = v^*$. Notice that regardless of the value of B, if at any time $v_1 > v_2$, (which is true initially), Z is a positive number, and v_1 will always be greater than v_2 for any finite time and single-valued particle growth rate.

This work was supported by the United States Nuclear Regulatory Commission under FIN A1412 and performed at Sandia National Laboratories, which is operated for the U. S. Department of Energy under Contract No. DE-AC04-76DP00789.

REFERENCES

Bassett, M. Gelbard, F., and Seinfeld, J. H. (1981). *Atmos. Environ.* 15:2395–2406.

Bergeron, K. D., Clauser, M. J., Harrison, B. D., Murata, K. K., Rexroth, P. E., Schelling, F. J., Sciacca, F. W., Senglaub, M., Shire, P. R., Trebilcock, W., and Williams, D. C. (1985). User's Manual for CONTAIN 1.0. SAND84-1204, NUREG/CR-4085, Sandia National Laboratories, Alburquerque, N.M.

Brock, J. R. (1971). *Atmos. Environ.* 5:833–841.

Brock, J. R. (1983). *Aerosol Sci. Technol.* 2:109–120.

Dunbar, I. H. (1985). Steam condensation modeling in aerosol codes. Final Report on Contract ECI-1232-B 7210-84-UK. U.K.A.E.A. Safety and Reliability Directorate, Culcheth, U.K.

Gelbard, F., and Seinfeld, J. H. (1980). *J. Colloid Interface Sci.* 78:485-501.

Gelbard, F., and Seinfeld, J. H. (1979). *J. Colloid, Interface Sci.* 68:173–183.

Gelbard, F. (1987). Aerosol growth in a nuclear reactor containment environment. Workshop on Water-Cooled Reactor Aerosol Code Evaluation and Uncertainity Assessment, September 9–11, SAND87-0943C. Commission of the European Communities, Brussels, Belgium.

Mason, B. J. (1971). *The Physics of Clouds*. 2nd ed. Claredon Press, Oxford, pp. 122–125.

Murata, K. K., Carroll, D. E., Washington, K. E., Schelling, F. J., Valdez, G. D., Williams, D. C., and Bergeron, K. D. (1989). User's Manual for CONTAIN 1.10: A Computer Code for Severe Nuclear Reactor Accident Containment Analysis, SAND87-2309, Sandia National Laboratories, Albuquerque, NM.

Pruppacher, H. R., and Klett, J. D. (1980). *Microphysics of Clouds and Precipitation*. D. Reidel, Dordrecht, Netherlands, pp. 412–420.

Warren, D. R., and Seinfeld, J. H. (1985). *Aerosol Sci. Technol.* 4:31–43.

Williams, M. M. R. (1983). *J. Colloid Interface Sci.* 93:252–263.

Received April 22, 1988, accepted August 25, 1988.